Journal of Theoretical and Applied Mechanics, Sofia, Vol.56 (2026) pp. 199-215
GENERAL MECHANICS

ON THE PROBLEM OF ENERGY DISSIPATION IN SPATIALLY MOVING MECHANISMS

V. RIZOV*,

Department of Technical Mechanics, University of Architecture, Civil Engineering and Geodesy, 1 Chr. Smirnensky blvd. 1046-Sofia, Bulgaria

[Received: 29 October 2025. Accepted: 26 May 2026]
doi: https://doi.org/10.55787/jtams.2026.2.AI00254

ABSTRACT: This paper is focused on analyzing the dissipated energy in mechanisms performing spatial motion. The components of the mechanisms are functionally graded along the length. Furthermore, the components have non-linear viscoelastic behavior. The viscoelastic behavior of the mechanism components is treated by a model having a spring and two dashpots (one of the dashpots has non-linear behavior). The viscoelastic model parameters and the specific mass change continuously along the length of the mechanism components. The dissipated energy is determined and checked by a method previously published. The influence of parameters of spatial motion and viscoelastic model parameters distribution on the dissipated energy is elucidated. An application of dissipated energy analysis using a failure criterion is presented.

KEY WORDS: spatial motion, energy dissipation, non-linear viscoelastic behaviour, functionally graded component.

1 INTRODUCTION

Functionally graded engineering materials, as a typical continuously inhomogeneous composite with smoothly changing properties in the solid, have attracted the attention of researchers and engineers in various fields of modern technology due to their exceptional mechanical properties [1–4]. These novel materials have broad application perspectives including in important areas such as aeronautical engineering, the automotive industry, and nuclear reactors [5–8]. In many applications, the functionally graded materials are utilized in key components exposed to extreme loads and influences [9–14]. Owing to their good performance under dynamic loads, functionally graded components are frequently employed in a variety of mechanisms.

Mechanisms performing different kinds of mechanical motion present important parts of various apparatuses, devices and machines used in modern engineering. In many applications these mechanisms execute spatial motion. Furthermore, the components of mechanisms usually move unevenly, which generates inertial loads on

*Corresponding author e-mail: v_rizov_fhe@uacg.bg

them. These inertia loads affect significantly the strength and fracture behavior of the mechanism components. Such important issues as safety, reliability and durability of mechanisms are also closely related to the impact of inertial loads on mechanism components. In some cases, when subjected to time-dependent inertial loads, these components behave as non-linear viscoelastic bodies. This circumstance shows that the analysis of various aspects of the nonlinear viscoelastic behavior of mechanism components is essential, especially in the context of their reliable functioning and safety. As is known, one of the general problems associated with viscoelastic deformation of engineering materials is energy dissipation [15–21]. The term "energy dissipation" refers to the loss of strain energy due to viscoelastic properties of materials. The correct estimation of the dissipated energy in structures and mechanisms under the impact of different loads is an important issue, mainly because it is related to the failure behavior. For instance, the energy dissipation reduces the risk of fracture in components of structures and mechanisms. Also, energy dissipation is one of the efficient factors in extending the life of structures and mechanisms. The importance of the energy dissipation problem is also confirmed by the fact that the number of scientific publications on this topic over the years is significant [15–21]. Although these publications contribute a lot to clarifying various aspects of energy dissipation, there are still questions that require more research efforts. One of these questions is the analysis of the dissipated energy in mechanisms performing spatial motion.

The basic purpose of this paper is to analyze the dissipated energy in spatially moving mechanisms with functionally graded components (the term "functionally graded component" can be used here, because the study accounts for the simultaneous variation of both physical property (specific mass) and mechanical performance (stiffness and damping)). The components of the mechanism have non-linear viscoelastic behavior. Furthermore, the components are functionally graded along their length. In particular, a mechanism with two components connected by a joint is considered in detail. The entire mechanism moves translationally along the axes of the spatial coordinate system. During the movement process, one of the components of the mechanism remains horizontal, while the other component also performs relative rotational movement in the joint. The law of motion (spatial translation and relative rotation) of the mechanism components is given. The acceleration and the inertia loads on the components are determined. The non-linear viscoelastic model used for analyzing the deformation of the components has a spring and two dashpots (one of the dashpots is with non-linear behavior). The stress-strain-time relation of the model is derived and applied for describing the non-linear viscoelastic deformation of the mechanism components. The parameters of this relation change continuously along the components length. The energy dissipation in the mechanism components is modeled through the dashpots. Therefore, the specific dissipated energy (SDE) is

found by analyzing the dashpots behavior. The dissipated energy in the mechanism is obtained by integrating the SDE over the volume of the mechanism components. An approach published early in the scientific literature is used for checking the dissipated energy obtained in this paper. The relation of the dissipated energy with the parameters of mechanism's motion and the change of parameters of the viscoelastic model along the length of mechanism's components is examined in detail and illustrated with various graphs. The approach developed in this paper can be used for dealing with the energy dissipation problem in mechanisms with functionally graded nonlinear viscoelastic components performing spatial motion. The findings presented here contribute to a better understanding of the phenomenon of energy dissipation. The main novel aspect of this paper is that the analysis encompasses the effects of factors such as spatial motion, continuous change of material properties, and nonlinear viscoelastic behavior on the dissipated energy in mechanisms. Regarding the novelty, it should also be specified that this paper investigates energy dissipation in mechanisms, unlike [21], where energy dissipation in beam structures is investigated.

2 Dissipation of Energy Analysis

2.1 Kinematic analysis

The mechanism depicted in Fig. 1 has two components, DH and HL, connected by a joint in point, H. These components represent inhomogeneous bars of nonlinear viscoelastic behavior. Bar, DH, moves translationally in the spatial coordinate system, xyz, according to the laws defined in Eqs. (1)

$$x_D = \beta t^3, \quad y_D = \delta t^3, \quad z_D = \lambda t^3\,, \tag{1}$$

where β, δ and λ are parameters, t is time, x_D, y_D and z_D are the coordinates of point, D. In the process of motion, bar, DH, remains horizontal. The other bar, HL, is involved in spatial translational motion together with bar, DH, and in the same time executes relative rotational motion around horizontal axis, y_2, according to the law presented in Eq. (2)

$$\varphi = \mu\, t\,, \tag{2}$$

where φ is the angle of rotation of HL, μ is a parameter (ϕ is depicted in Fig. 1). The axis, y_2, passes through point, H, and is parallel to axis, y_1, as shown in Fig. 1.

The mechanism is under inertia loads induced by the acceleration. Since bar, DH, is moving translationally, every point on it has the same acceleration. The projections of this acceleration, a_{Bx_1}, a_{By_1} and a_{Bz_1}, along axes, x_1, y_1 and z_1, are found by Eqs. (3) (axes, x_1, y_1 and z_1, are defined in Fig. 1)

$$a_{By_1} = \frac{d^2 x_D}{dt^2} = 6\beta t\,, \quad a_{By_1} = \frac{d^2 y_D}{dt^2} = 6\delta t\,, \quad a_{Bz_1} = \frac{d^2 z_D}{dt^2} = 6\lambda t\,. \tag{3}$$

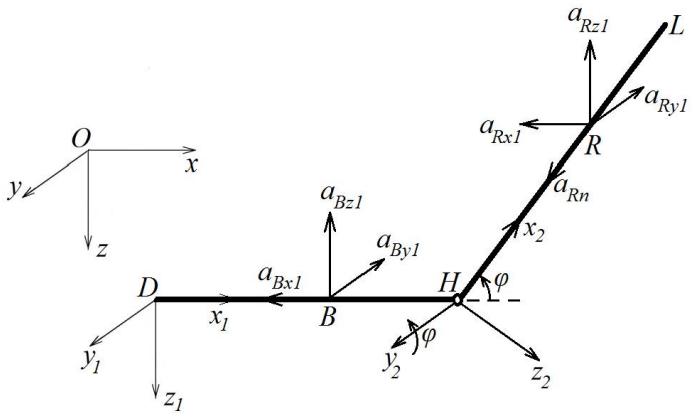

Figure 1. Mechanism schema.

These projections are depicted in an arbitrary point, B, on the bar, DH, as shown in Fig. 1.

The acceleration, $\vec{a}_R$, of an arbitrary point, R, on bar, HL, is expressed in Eq. (4)

$$\vec{a}_R = \vec{a}_{Rtr} + \vec{a}_{Rrt}\,, \tag{4}$$

where $\vec{a}_{Rtr}$ and $\vec{a}_{Rrt}$ are the accelerations due to translational and rotational motions, respectively.

Equation (5) is used for obtaining of $\vec{a}_{Rtr}$, i.e.

$$\vec{a}_{Rtr} = \vec{a}_{Rx_1} + \vec{a}_{Ry_1} + \vec{a}_{Rz_1}\,, \tag{5}$$

where

$$a_{Rx_1} = a_{Bx_1}\,, \quad a_{Ry_1} = a_{By_1}\,, \quad a_{Rz_1} = a_{Bz_1}\,. \tag{6}$$

Accelerations, a_{Bx_1}, a_{By_1} and a_{Bz_1}, are determined by Eqs. (3).

The acceleration of point, R, due to rotational motion is derived by Eq. (7)

$$\vec{a}_{Rrt} = \vec{a}_{Rn}\,, \tag{7}$$

where $\vec{a}_{Rn}$ is the normal acceleration found by Eq. (8)

$$a_{Rn} = \omega_{rn}^2 x_2\,, \quad 0 \le x_2 \le l_2\,. \tag{8}$$

Here, x_2 is the longitudinal axis of the bar, HR, as shown in Fig. 1, l_2 is the length of bar. The angular velocity, ω_{rn}, of bar, HR, is determined by using Eq. (9)

$$\omega_{rn} = \frac{d\varphi}{dt} = \mu\,. \tag{9}$$

The accelerations, a_{Rx_1}, a_{Ry_1}, a_{Rz_1} and a_{Rn}, are depicted in point, R, on bar, HR, in Fig. 1.

2.2 Determination of inertia loads

The intensities, φ_{Bx_1}, φ_{By_1} and φ_{Bz_1}, of the inertia loads parallel to axes, x_1, y_1 and z_1, in an arbitrary point, B, of bar, DH, are written in Eqs. (10)

$$\varphi_{Bx_1} = -ma_{Bx_1}\,, \quad \varphi_{By_1} = -ma_{By_1}\,, \quad \varphi_{Bz_1} = -ma_{Bz_1}\,. \tag{10}$$

In the above equations, m, is the specific mass, i.e. the mass per unit length. The bar is continuously inhomogeneous along the length. That's why m changes continuously along the length. This change is described by the law written in Eq. (11)

$$m = m_D + \frac{m_H - m_D}{l_1^{\theta_1}} x_1^{\theta_1}\,, \quad 0 \le x_1 \le l_1\,. \tag{11}$$

Here, x_1 is the longitudinal axis of the bar, l_1 is the length, m_D and m_H are the specific masses in points, D and H, respectively, θ_1 is a parameter.

The intensities, φ_{Bx_1}, φ_{By_1} and φ_{Bz_1}, are directed opposite to accelerations, a_{Bx_1}, a_{By_1} and a_{Bz_1}, respectively.

Equations (12) are applied to derive the intensities, φ_{Rx_1}, φ_{Ry_1}, φ_{Rz_1}, and φ_{Rn}, of inertia load in an arbitrary point, R, in bar, HL

$$\varphi_{Rx_1} = -m_{HL}a_{Rx_1}\,, \quad \varphi_{Ry_1} = -m_{HL}a_{Ry_1}\,, \quad \varphi_{Rz_1} = -m_{HL}a_{Rz_1}\,, \quad \varphi_{Rn} = -m_{HL}a_{Rn}\,. \tag{12}$$

Here, m_{HL} is the specific mass. Equation (11) is used for describing the change of m_{HL} along the length. In this connection, l_1, m_D, m_H, x_1 and θ_1 are replaced with l_2, m_{Hr}, m_L, x_2 and θ_2 where m_{Hr} and m_L are the specific masses in points, H and L, of the bar, θ_2 is a parameter. The intensities, φ_{Rx1}, φ_{Ry1}, φ_{Rz1} and φ_{Rn}, are directed opposite to accelerations, a_{Rx_1}, a_{Ry_1}, a_{Rz_1} and a_{Rn}, respectively.

2.3 Determination of dissipated energy

The dissipated energy, U_{dDH}, in bar, DH, is found by Eq. (13)

$$U_{dDH} = \iiint\limits_{(V_{DH})} u_{0d}\mathrm{d}V\,, \tag{13}$$

where u_{0d} is the SDE in the dashpots of the viscoelastic model, V_{DH} is the volume of the bar. The SDE is obtained by Eq. (14)

$$u_{0d} = \int\limits_0^{\varepsilon} \sigma \mathrm{d}\varepsilon\,, \tag{14}$$

where σ and ε are the stress and strain induced by the inertia loads.

2.4 VISCOELASTIC MODEL

The schema of the viscoelastic model used for treating the behavior of the bar under inertia loads is depicted in Fig. 2. The model has a linear-elastic spring with modulus, E, a dashpot of linear behavior with coefficient of viscosity, η, and a dashpot of non-linear behavior (this dashpot is marked by (nl) as shown in Fig. 2.

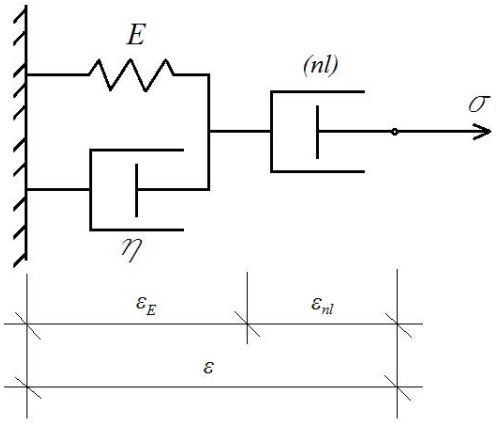

Figure 2. Viscoelastic model.

The strains in the spring and in the dashpot of linear behavior are marked by ε_E and ε_η, respectively (Fig. 2). Apparently,

$$\varepsilon_\eta = \varepsilon_E \,. \tag{15}$$

The strain in the dashpot of non-linear behavior is marked by ε_{nl} as shown in Fig. 2. The strain in the model, ε, is obtained by Eq. (16)

$$\varepsilon = \varepsilon_E + \varepsilon_{nl} \,. \tag{16}$$

The stresses in the spring and the dashpot of linear behavior are marked by σ_E and σ_η, respectively. These stresses are related with ε_E and ε_η, by using Eqs. (17)

$$\sigma_E = E\varepsilon_E \,, \quad \sigma_\eta = \eta\dot{\varepsilon}_\eta \,. \tag{17}$$

The stress in dashpot of non-linear behavior is marked by σ_{nl}. Equation (18) is applied for expressing of σ_{nl} through $\dot{\varepsilon}_{nl}$.

$$\sigma_{nl} = P\dot{\varepsilon}_{nl}^{s} \,, \tag{18}$$

where P and s are parameters, $\dot{\varepsilon}_{nl}$ is the time derivative.

The model is loaded by stress, σ_{vm}, written in Eq. (19)

$$\sigma = \psi_1 t\,, \tag{19}$$

where ψ_1 is a parameter.

Apparently,

$$\sigma_{nl} = \sigma\,. \tag{20}$$

From Eqs. (18), (19) and (20), we have

$$P\dot{\varepsilon}_{nl}^{s} = \psi_1 t\,. \tag{21}$$

From Eq. (21) we obtain

$$\int_0^{\varepsilon} \mathrm{d}\varepsilon_{nl} = \int_0^{t} \left(\frac{\psi_1 t}{P}\right)^{\frac{1}{s}} \mathrm{d}t\,. \tag{22}$$

By performing integration in Eq. (22) we derive

$$\varepsilon_{nl} = \frac{\psi_1^{\frac{1}{s}} t^{\frac{1+s}{s}} s}{P^{\frac{1}{s}}(1+s)}\,. \tag{23}$$

The equilibrium of the viscoelastic model in Fig. 2 indicates that

$$\sigma_{\eta} + \sigma_E = \sigma\,. \tag{24}$$

From Eqs. (15), (17), (19) and (24), we have

$$\eta\dot{\varepsilon}_E + E\varepsilon_E = \psi_1 t\,. \tag{25}$$

The solution of differential Eq. (25) is written as

$$\varepsilon_E = C_1 e^{-\zeta t} + \bar{\varepsilon}_E\,, \tag{26}$$

where

$$\zeta = \frac{E}{\eta}\,. \tag{27}$$

In Eq. (26), C_1 is integration constant, $\bar{\varepsilon}_E$ is a particular solution of Eq. (26). This solution is written in Eq. (28).

$$\bar{\varepsilon}_E = \beta_1 t + \beta_2\,, \tag{28}$$

where constants, β_1 and β_2, are determined by replacing of ε_E and $\dot{\varepsilon}_E$ with $\bar{\varepsilon}_E$ and $\dot{\bar{\varepsilon}}_E$ in Eq. (25). This leads to the following equation:

$$\beta_1 + \beta_2\zeta + \beta_1\zeta t = \frac{\psi_1}{\eta}t\,. \tag{29}$$

From Eq. (29), we derive

$$\beta_1 = \frac{\psi_1}{E}\,, \tag{30}$$

$$\beta_2 = -\frac{\psi_1}{\zeta E}\,. \tag{31}$$

Eqs. (30) and (31) are inserted in Eq. (29), i.e.

$$\varepsilon_E = C_1 e^{-\zeta t} + \frac{\psi_1}{E}\Big(t - \frac{1}{\zeta}\Big). \tag{32}$$

The constant, C_1, is determined from the following condition:

$$\varepsilon_E\,(0) = 0\,. \tag{33}$$

After substituting of $t = 0$ in Eq. (33), we derive

$$C_1 = \frac{\psi_1}{\zeta\, E}\,. \tag{34}$$

Thus, Eq. (32) is rewritten as

$$\varepsilon_E = \frac{\psi_1}{\zeta\, E}e^{-\zeta t} + \frac{\psi_1}{E}\Big(t - \frac{1}{\zeta}\Big). \tag{35}$$

Finally, Eqs. (23) and (35) are inserted in Eq. (16). This leads to the following expression:

$$\varepsilon = \frac{\psi_1}{\zeta\, E}e^{-\zeta t} + \frac{\psi_1}{E}\Big(t - \frac{1}{\zeta}\Big) + \frac{\psi_1^{\frac{1}{s}} t^{\frac{1+s}{s}} s}{P^{\frac{1}{s}}(1+s)}\,. \tag{36}$$

We combine Eqs. (19) and (36) and perform mathematical transformations. This leads to the following result:

$$\varepsilon = \frac{\sigma}{\zeta\, Et}\Big(e^{-\zeta t} - 1\Big) + \frac{\sigma}{E} + \frac{\sigma^{\frac{1}{s}} st}{P^{\frac{1}{s}}(1+s)}\,. \tag{37}$$

Equation (37) represents the stress-strain-time relationship applied for treating the non-linear viscoelastic behavior of bar, DH, under inertia loads. Since the bar is continuously inhomogeneous along the length, the parameters, E, η, P and s, change along axis, x_1, obeying the laws defined in Eqs. (38) and (39)

$$E = E_D + \frac{E_H - E_D}{l_1^{\theta_3}} x_1^{\theta_3}\,, \qquad \eta = \eta_D + \frac{\eta_H - \eta_D}{l_1^{\theta_4}} x_1^{\theta_4}\,, \tag{38}$$

$$P = P_D + \frac{P_H - P_D}{l_1^{\theta_5}} x_1^{\theta_5}\,, \qquad s = s_D + \frac{s_H - s_D}{l_1^{\theta_6}} x_1^{\theta_6}\,, \tag{39}$$

where

$$0 \leq x_1 \leq l_1\,. \tag{40}$$

In Eqs. (38) and (39), E_D, η_D, P_D and s_D are the values of E, η, P and s in point, D, of the bar, E_H, η_H, P_H and s_H are the values of E, η, P and s in point, H, of the bar, θ_3, θ_4, θ_5 and θ_6 are parameters.

2.5 Analysis of mechanism components under inertia loads

The inertia loads acting on bar, DH, induce in each cross-section bending moments around the horizontal and vertical centric axes and an axial force. Therefore, the change of the strain, ε, in an arbitrary cross-section is presented by Eqs. (41)

$$\varepsilon = \varepsilon_C + \kappa_{yC} y_C + \kappa_{zC} z_C\,,$$
$$-\frac{b_1}{2} \leq y_C \leq \frac{b_1}{2}\,, \qquad -\frac{h_1}{2} \leq z_C \leq \frac{h_1}{2}\,. \tag{41}$$

In Eqs. (41), ε_C is the strain in the centre of the cross-section, k_{yC} and κ_{zC} are the bar curvatures, y_C and z_C are the horizontal and vertical centric axes of the cross-section (y_C and z_C are parallel to y_1 and z_1, respectively), b_1 and h_1 are the width and thickness of the cross-section. The quantities, ε_C, k_{yC} and κ_{zC}, are determined by Eqs. (42)

$$N = \iint\limits_{(A_{DH})} \sigma \mathrm{d}A\,, \quad M_{yC} = \iint\limits_{(A_{DH})} \sigma z_C \mathrm{d}A\,, \quad M_{zC} = \iint\limits_{(A_{DH})} \sigma y_C \mathrm{d}A\,, \tag{42}$$

where A_{DH} is the area of the cross-section, N, M_{yC} and M_{zC} are the axial force and bending moments around axes, y_C and z_C. The quantities, N, M_{yC} and M_{zC}, in an arbitrary cross-section located at distance, s_1, from point, D, are determined by

reduction of the inertia loads through Eqs. (43) and (44)

$$N = \int_{s_1}^{l_1} \varphi_{Bx_1} \mathrm{d}x_1 + H_{x_1}\,, \quad M_{yC} = \int_{s_1}^{l_1} \varphi_{Bz_1}(x_1 - s_1)\mathrm{d}x_1 + H_{z_1}(l_1 - s_1)\,, \tag{43}$$

$$M_{zC} = \int_{s_1}^{l_1} \varphi_{By_1}(x_1 - s_1)\mathrm{d}x_1 + H_{y_1}(l_1 - s_1)\,, \tag{44}$$

where H_{x_1}, H_{y_1} and H_{z_1} are the reactions in the joint in point, H (H_{x_1}, H_{y_1} and H_{z_1} are parallel to axes, x_1, y_1 and z_1, respectively). The reactions are found by analyzing the equilibrium of bar, HL, through equations $\sum F_{ix_1} = 0$, $\sum F_{iy_1} = 0$ and $\sum F_{iz_1} = 0$. These equations lead to the following expressions for H_{x_1}, H_{y_1} and H_{z_1}:

$$H_{x_1} = \int_0^{l_2} (-\varphi_{Rx_1} - \varphi_{Rn}\cos\phi)\mathrm{d}x_2\,, \quad H_{y_1} = \int_0^{l_2} (-\varphi_{Ry_1})\mathrm{d}x_2\,, \tag{45}$$

$$H_{z_1} = -\int_0^{l_2} (-\varphi_{Rz_1} + \varphi_{Rn}\sin\phi)\mathrm{d}x_2\,. \tag{46}$$

Equations (42) can be used to determine ε_C, k_{yC} and κ_{zC} in any cross-section of bar, DH, by the MatLab.

In the model depicted in Fig. 2, energy is dissipated by the two dashpots. Therefore, Eq. (14) is transformed as

$$u_{0d} = \int_0^{\varepsilon_\eta} \sigma_\eta \mathrm{d}\varepsilon_\eta + \int_0^{\varepsilon_{nl}} \sigma_{nl}\mathrm{d}\varepsilon_{nl}\,. \tag{47}$$

The dissipated energy in bar, DH, is found by Eq. (13). The integration is performed by the MatLab.

The behavior of bar, HL, is treated by the model in Fig. 2. The thickness and width of this bar are denoted by h_2 and b_2, respectively. Equations (38) and (39) are used to present the change of E, η, P and s along the length of the bar. In this relation, E_D, η_D, P_D, s_D, E_H, η_H, P_H, s_H, θ_3, θ_4, θ_5, θ_6 and x_1 are replaced with E_{Hr}, η_{Hr}, P_{Hr}, s_{Hr}, E_L, η_L, P_L, s_L, θ_7, θ_8, θ_9, θ_{10} and x_2 in Eqs. (38) and (39). Here, E_{Hr}, η_{Hr}, P_{Hr}, s_{Hr} are the values of E, η, P and s in point, H, of bar, HL, E_L, η_L, P_L and s_L are the values of E, η, P and s in point, L, of the bar, θ_7, θ_8, θ_9, θ_{10} are parameters.

The quantities, ε_C, k_{yC} and κ_{zC}, in an arbitrary cross-section of the bar, HL, are determined by Eqs. (42). The axial force and the bending moments involved in Eqs. (42) are obtained by reduction of the inertial loads through Eqs. (48), (49) and (50)

$$N = \int_{s_2}^{l_2} \varphi_{Rx_1} \cos\phi - \varphi_{Rz_1} \sin\phi + \varphi_{Rn}) \mathrm{d}x_2 \,, \tag{48}$$

$$M_{yC} = \int_{s_2}^{l_2} [-\varphi_{Rx_1} \sin\phi(x_2 - s_2) - \varphi_{Rz_1} \cos\phi(x_2 - s_2)\,] \,\mathrm{d}x_2 \,, \tag{49}$$

$$M_{zC} = \int_{s_2}^{l_2} [-\varphi_{Ry_1}(x_2 - s_2)] \,\mathrm{d}x_2 \,, \tag{50}$$

where s_2 is the distance between the cross-section and point, H. The dissipated energy, U_{dHL}, in bar, HL, is found by integrating the SDE in the bar volume. Finally, the dissipated energy, U_d, in the mechanism in Fig. 1 is determined by using Eq. (51)

$$U_d = U_{dDH} + U_{dHL} \,. \tag{51}$$

The dissipated energy thus determined is checked by the approach published in [18]. This approach is based on calculation of the SDE in the dashpots through Eq. (52)

$$u_{0d} = \int_0^t \sigma_\eta \dot{\varepsilon}_\eta \mathrm{d}t + \int_0^t \sigma_{nl} \dot{\varepsilon}_{nl} \mathrm{d}t \,. \tag{52}$$

By performing the mathematical manipulations in Eq. (52) and integrating the SDE over the volume of the mechanism components, we derive dissipated energy agreeing very well with the results obtained in the present study.

3 Parametric Study

Here we study the effects of motion, inhomogeneity and sizes of the bars on the dissipated energy in the mechanism. In this relation, we apply the solution of the dissipated energy obtained in Section 2 of this paper. The study is carried-out by using the following data:

$$b_1 = 0.012 \text{ m}, \quad h_1 = 0.018 \text{ m}, \quad l_1 = 0.300 \text{ m}, \quad b_2 = 0.015 \text{ m},$$

$$h_2 = 0.020 \text{ m}, \quad l_2 = 0.800 \text{ m}, \quad \theta_1 = 0.6, \quad \theta_2 = 0.6,$$
$$\theta_3 = 0.6, \quad \theta_4 = 0.7, \quad \theta_5 = 0.7, \quad \theta_6 = 0.7,$$
$$\theta_7 = 0.7, \quad \theta_8 = 0.8, \quad \theta_9 = 0.8, \quad \theta_{10} = 0.8\,.$$

The effects studied are illustrated by the graphs reported in Figs. 3, 4, 5, 6 and 7.

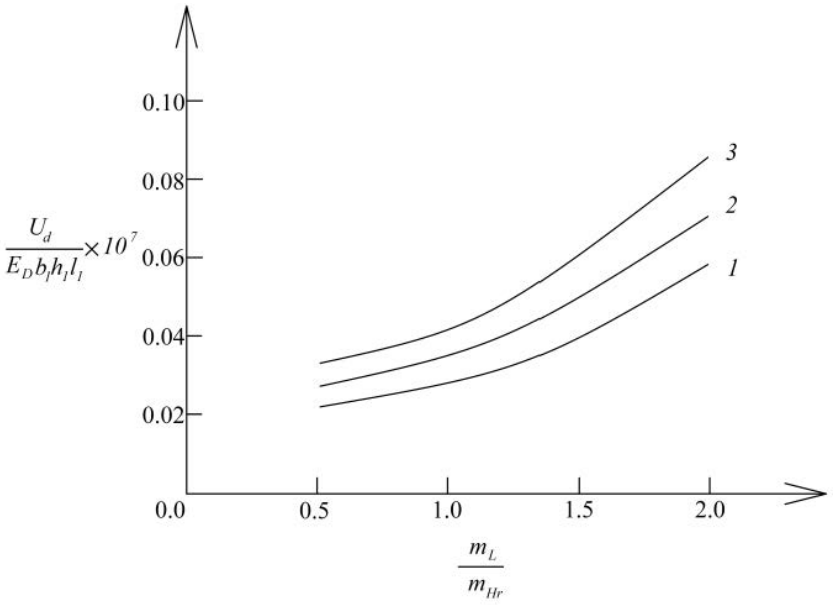

Figure 3. The non-dimensional dissipated energy as function of m_L/m_{Hr} ratio (curve 1 – at $\beta = 0.2$, curve 2 – at $\beta = 0.4$ and curve 3 – at $\beta = 0.6$).

Consider the graphs in Fig. 3. They illustrate how the dissipated energy is affected by the parameter, β, of the motion along axis, x, and m_L/m_{Hr} ratio (this ratio characterizes the change of m_{HL} along the length of bar, HL). The dissipated energy in Fig. 3 is presented in non-dimensional form.

The graphs indicate that the dissipated energy grows as a result of increase of the value of the parameter, β. Growth of the dissipated energy is induced also by rise of the ratio, m_L/m_{Hr} (Fig. 3).

One can observe how the dissipated energy is affected by η_H/η_D ratio at various values of parameter, δ, in Fig. 4 (ratio, η_H/η_D, and parameter, δ, characterize the change of η along the length of bar, DH, and the motion of the mechanism along axis, y, respectively). It can be seen in Fig. 4 that rise of ratio, η_H/η_D, results in growth of the dissipated energy. A similar effect on dissipated energy, i.e. growth, is also caused by the increase in the parameter, δ.

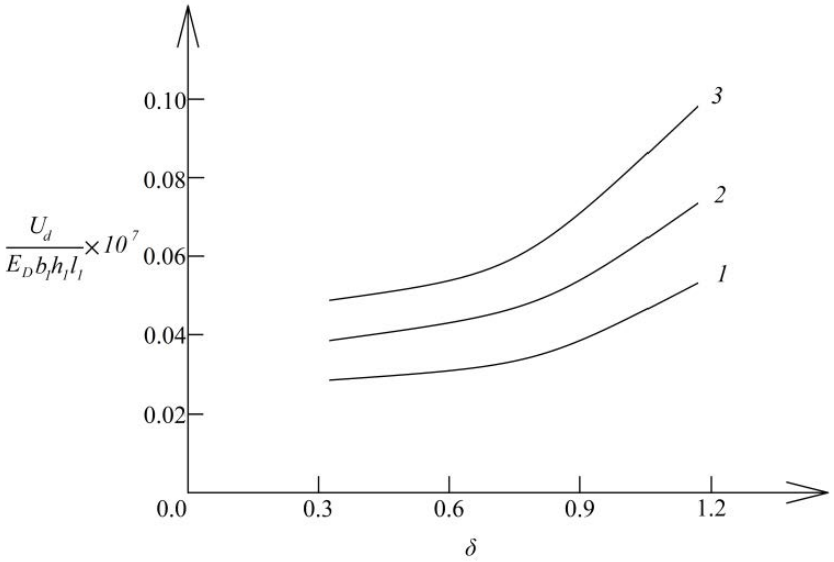

Figure 4. The effect of δ on non-dimensional dissipated energy (curve 1 – at $\eta_H/\eta_D = 0.5$, curve 2 – at $\eta_H/\eta_D = 1.0$ and curve 3 – at $\eta_H/\eta_D = 2.0$).

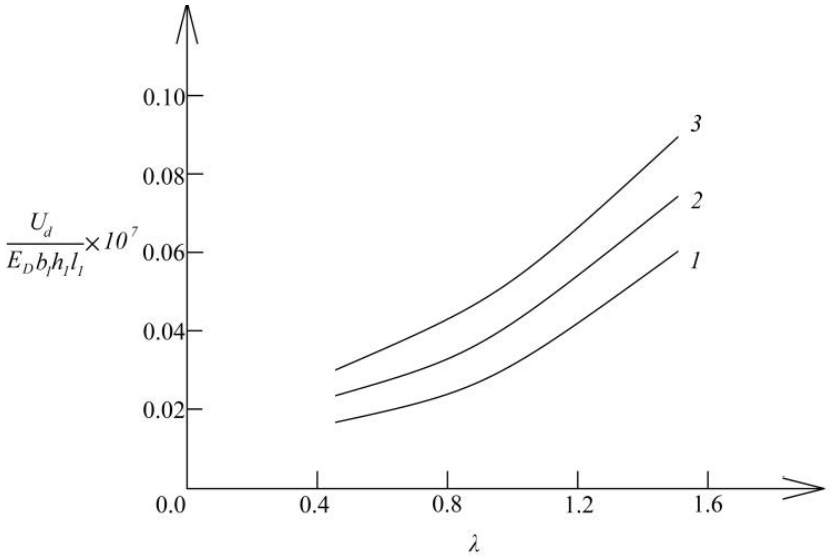

Figure 5. The influence of λ on non-dimensional dissipated energy (curve 1 – at $m_H/m_D = 0.5$, curve 2 – at $m_H/m_D = 1.0$ and curve 3 – at $m_H/m_D = 2.0$).

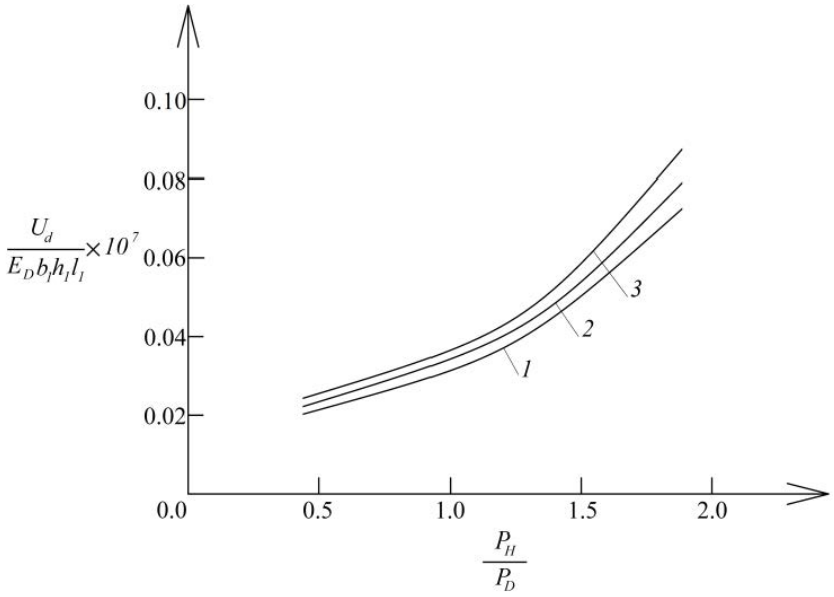

Figure 6. The non-dimensional dissipated energy vs. P_H/P_D ratio (curve 1 – at $\mu = 0.6$, curve 2 – at $\mu = 1.2$ and curve 3 – at $\mu = 1.8$).

We study further how the dissipated energy is affected by the change of the specific mass along the length of bar, DH, and the motion of the mechanism along the vertical axis, z. In this relation, the effects of the change of m_H/m_D ratio and increase of parameter, λ, on the DE are investigated. The findings of the investigation are illustrated by the graphs in Fig. 5. The inspection of these graphs reveals that the dissipated energy grows when m_H/m_D ratio increases. Growth of the dissipated energy is induced also by rise of the value of parameter, λ (Fig. 5).

One can examine in Fig. 6 the effect of P_H/P_D ratio on the DE (ratio, P_H/P_D, characterizes the change of P along the length of bar, DH). The effect of the rotation of bar, HL, around point, H (the rotation is characterized by parameter, μ) on the dissipated energy can also be examined in Fig. 6. The increase of μ causes growth of dissipated energy (Fig. 6). Growth of the dissipated energy is caused also by increase of P_H/P_D ratio (Fig. 6).

It is explored also how the dissipated energy is influenced by the values of parameters, θ_1 and θ_3. The influence of these parameters can be seen in Fig. 7. It can be observed that using of high values of θ_1 and θ_3 leads to significant increase of the dissipated energy (Fig. 7). Another issue that is explored here is how the present analysis of the dissipated energy can be applied in the engineering practice. In this

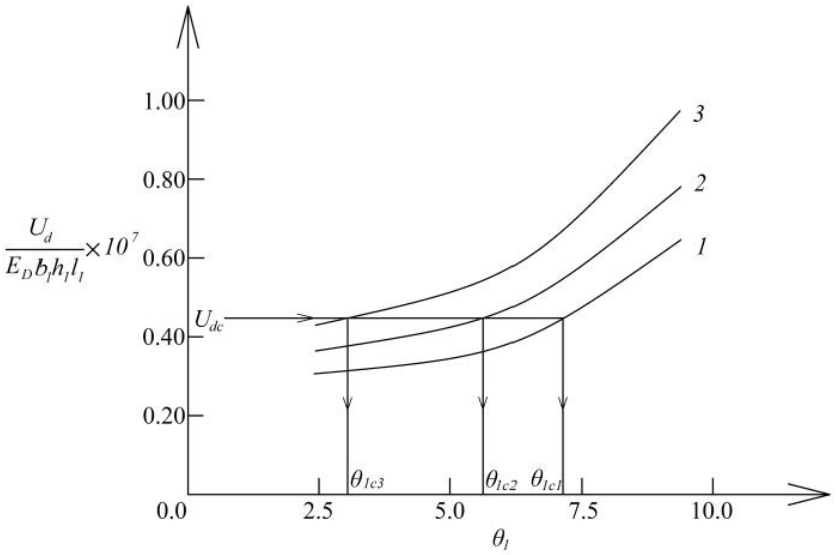

Figure 7. Change of the non-dimensional dissipated energy with increase of θ_1 (curve 1 – at $\theta_3 = 2$, curve 2 – at $\theta_3 = 4$ and curve 3 – at $\theta_3 = 6$).

regard, the following failure criterion can be used:

$$U_d = U_{dc}\,, \tag{53}$$

where U_{dc} is the limit value of the dissipated energy. The physical meaning of (53) is that when U_d exceeds U_{dc}, failure due to thermal degradation or fatigue-induced fracture will occur in the components of the mechanism. Criterion (53) is applied to determine the boundary value, θ_{1c}, of parameter θ_1 at three values of θ_3 in Fig. 7. One can see in Fig. 7 that the θ_{1c} decreases with increase of θ_3 (this is explained by an increase in U_d as a result of an increase in θ_3).

4 Conclusions

An approach for treating the problem of energy dissipation in mechanisms that move spatially is developed. In particular, a mechanism with two functionally graded components which behave as non-linear viscoelastic bodies is considered. The whole mechanism moves translationally along the axes of the spatial rectangular coordinate system. Simultaneously, one of the components performs relative rotational motion. The analysis sheds light on the relationship between the dissipated energy and such factors as parameters of motion and distribution of material properties in the components of the mechanism. It is found that the dissipated energy grows as a

result of increase of the parameters, β, δ, λ, and μ, of the motion of the mechanism. Growth of the dissipated energy is established also as a result of rise of the ratios of specific masses, m_L/m_{Hr} and m_H/m_D. The effects of the nonlinear viscoelastic model parameters on the dissipated energy are also evaluated. The analysis shows that the dissipated energy increases as a result of growth of η_H/η_D and P_H/P_D ratios. The conclusion that can be made is that the spatial distribution of mass shifts the "damping center" of the bars, leading to more efficient energy absorption in specific segments. From view-point of the engineering practice, this paper contributes for deepening the knowledge for the energy dissipation which is of great importance at evaluation of durability and fracture performance of spatially moving functionally graded mechanisms having viscoelastic behavior. An example of a practical application of the present analysis is shown for determining the boundary value of the θ_1 parameter using a failure criterion. It should be underlined that the approach developed in this paper can be used to analyze the dissipated energy in more complex configurations performing spatial motion, provided that the analytical expressions of the laws of motion are known. Furthermore, the viscoelastic models and the variation of material properties in the mechanism components can be arbitrary. Finally, it can be said that this article provides a theoretical basis for studying the dissipated energy in components of spatially moving mechanisms.

REFERENCES

[1] M. GASIK (2010) Functionally graded materials: bulk processing techniques. *International Journal of Materials and Product Technology* **39** 20-29.

[2] G. UDUPA, S. SHRIKANTHA RAO, K. RAO GANGADHARAN (2014) Functionally Graded Composite Materials: An Overview. *Procedia Materals Science* **5** 1291-1299.

[3] S. BOHIDAR, R. SHARMA, P. MISHRA (2014) Functionally graded materials: A critical review. *International Journal of Research* **1** 289-301.

[4] V. RIZOV (2024) Adhesively bonded inhomogeneous viscoelastic beam of cruciform cross-section: A delamination study. *AIP Conference Proceedings* **2980** 050009.

[5] M. EL-WAZERY, A. EL-DESOUKY (2015) A review on functionally graded ceramic-metal materials. *Material Environment Science* **6** 1369-1376.

[6] M. NAEBE, K. SHORVANIMOGHADDAM (2016) Functionally graded materials: A review of fabrication and properties. *Applied Materials Today* **5** 223-245.

[7] R. MAHAMOOD, E. AKINLABI (2017) "Functionally Graded Materials". Springer.

[8] V. RIZOV (2017) An analytical solution to the stain energy release rate of a crack in functionally graded nonlinear elastic beams. *European Journal of Mechanics, A/Solids* **65** 301-312.

[9] A. REICHARDT, ET AL. (2021) Advances in additive manufacturing of metalbased functionally graded materials. *International Materials Reviews* **66** 1-29.

[10] A. SAIYATHIBRAHIM, R. SUBBRAMANIYAN, P. DHANAPL (2016) Centrefugally cast functionally graded materials – review. In: International Conference on Systems, Science, Control, Communications, Engineering and Technology, 68-73.

[11] S. SHRIKANTHA RAO, K.V. GANGADHARAN (2014) Functionally graded composite materials: an overview. *Procedia Materials Science* **5** 1291-1299.

[12] S. SURESH, A. MORTENSEN (1998) "Fundamentals of functionally graded materials". IOM Communications Ltd, Londo.

[13] A.J. MARKWORTH, K.S. RAMESH JR., W.P. PARKS (1995) Review: modeling studies applied to functionally graded materials. *Journal of Materials Science* **30** 2183-2193.

[14] R.J. BUTCHER, C.E. ROUSSEAU, H.V. TIPPUR (1999) A functionally graded particulate composite: Measurements and Failure Analysis. *Acta Materialia* **47** 259-268.

[15] J.G. WILLIAMS (1973) "Stress analysis of polymers". Longman Group Ltd.

[16] A. BLAKE (1985) "Handbook of mechanics, materials and structures", John Wiley & Sons.

[17] R. MALENOV, R. KURKCHIEV, V. ALEXANDROV (1986)"Theoretical Mechanic", Technique.

[18] I. NARISAWA (1987) "Strength of polymer materials". Chemistry.

[19] K. MLADENOW, V. RIZOV (2001) "Theoretical mechanics – Part II – Dynamics". ABC Technique.

[20] N. DOWLING (2013) "Mechanical behavior of materials". Springer.

[21] V. RIZOV (2021) Energy dissipation in viscoelastic multilayered inhomogeneous beam structures: an analytical study. *Materials Science Forum* **1046** 39-44.